Current Applied Physics 13 (2013) 1383–1390

Contents lists available at SciVerse ScienceDirect

Current Applied Physics

journal homepage: www.elsevier.com/locate/cap

Comparison of physicochemical properties of bio and commercial hydroxyapatite

A.L. Giraldo-Betancur [a], D.G. Espinosa-Arbelaez [b,c], A. del Real-López [c], B.M. Millan-Malo [c], E.M. Rivera-Muñoz [c], E. Gutierrez-Cortez [d], P. Pineda-Gomez [e,f], S. Jimenez-Sandoval [a], M.E. Rodriguez-García [c,*]

[a] Centro de Investigación y de Estudios Avanzados del IPN, Unidad Querétaro, Apartado Postal 1-798, Querétaro, Qro. C.P. 76001, Mexico
[b] Posgrado en Ciencia e Ingeniería de Materiales, Instituto de investigaciones en Materiales, Universidad Nacional Autónoma de México, Campus Juriquilla, Querétaro, Qro., Mexico
[c] Departamento de Nanotecnología, Centro de Física Aplicada y Tecnología Avanzada, Universidad Nacional Autónoma de México, Campus Juriquilla, Querétaro, Qro., Mexico
[d] División de Investigación y Posgrado, Facultad de Ingeniería, Universidad Autónoma de Querétaro, Querétaro, Qro., Mexico
[e] Facultad de Ciencias Exactas y Naturales, Universidad de Caldas, Sede Central, Calle 65 No. 26-10, Apartado aéreo 275, Manizales, Caldas, Colombia
[f] Facultad de Ciencias Exactas y Naturales, Universidad Nacional de Colombia Sede Manizales, Cra 27 No. 64-60, Apartado aéreo 127, Manizales, Caldas, Colombia

ARTICLE INFO

Article history:
Received 29 January 2013
Received in revised form
2 April 2013
Accepted 12 April 2013
Available online 24 April 2013

Keywords:
Bio-hydroxyapatite
Commercial-hydroxyapatite
Thermal degradation
Crystallinity
Organic material

ABSTRACT

This article reports a physicochemical comparison of synthetic and biological Hydroxyapatite (HAp). Eight samples were separated into two groups: bio and commercial hydroxyapatite (bio-HAp and commercial-HAp). The bio-HAp group containing *defat*, *alkaline*, and *calcined* samples taken from bovine bone were obtained by using three different treatments, in order to establish their effect on the final product quality. The commercial-HAp group, from different sources: *NIST*, *sigma*, *apafill G*, *coralina*, and *biograft*, were analyzed and compared with the bio-HAp results. Thermogravimetric analysis (TG) was used in order to establish thermal degradation of the samples; structural behavior was then analyzed by X-Ray Diffraction (XRD) to found the crystalline phases, as well as the crystalline quality. Fourier Transform Infrared Spectroscopy (FTIR) was performed in order to identify the corresponding HAp functional groups within the samples. The surface morphology was analyzed by Scanning Electron Microscopy (SEM) and the elemental composition was established by using Inductively Coupled Plasma Optical Emission Spectroscopy (ICP-OES). It was found that the calcination process obtains HAp with comparable quality to the commercial samples. A crystallinity greater than 62% after the *alkaline* process was found. Additionally, the surface of the *alkaline* sample presents a transition behavior between dense and porous morphology.

1. Introduction

Bone is a living tissue, which is basically composed of an organic phase (20–30 wt%), an inorganic phase (60–70 wt%) and around 5 wt% of water. The organic matrix is composed mainly of collagen, but there are other compounds in small concentrations, such as lipids and non-collagenous proteins. The organic phase provides elasticity, flexibility, and resistance to the bone. On the other hand, hydroxyapatite (HAp) – chemical formula $Ca_{10}(PO_4)_6(OH)_2$ – is the main component of the inorganic matrix. There are other ions, such as magnesium, fluoride, and sodium that form the minor components of the inorganic matrix; the whole matrix gives hardness and stiffness to the bone [1–6].

The understanding of both bone components is important for biomedical applications such as prosthesis and partial bone replacement among others [3,7–9]. The main component of the inorganic matrix (HAp) has gained significant attention due to its excellent biocompatibility, bioactivity, non-inflammatory behavior, non-immunogenicity, and high osteoconductive and/or osteoinductive nontoxicity properties, as well as its easy processing [3,4,10–12]. Thanks to these properties, HAp has been widely used in dental applications and hard tissue surgery, in part due to its ability to bond with bone tissue after the procedure [13–15].

* Corresponding author. Tel.: +52 442 2381141.
E-mail addresses: marioga@fata.unam.mx, mariorodga@gmail.com (M.E. Rodriguez-García).

1567-1739/$ – see front matter © 2013 Elsevier B.V. All rights reserved.
http://dx.doi.org/10.1016/j.cap.2013.04.019

However, HAp does not have the required mechanical properties for such applications; typically, its use demands the capacity to bear a high load. In relation to this point it is important to note that there have been many attempts to reinforce and combine HAp with other ceramics, polymers and bioactive glasses in order to improve the mechanical and biological properties through a composite of materials [14,16].

HAp can be obtained from natural and synthetic sources, and these have been used for bone replacement and ingrowth. The synthetic HAp has a stoichiometric distribution of its components; for this reason it does not have the same mineral traces of natural bone. The mineral traces play an important role in the osteointegration process. Therefore, HAp from natural sources, e.g., coral and bovine bone is more similar to human bone tissue. Synthetic HAp, unlike HAp from natural sources (bio-HAp), does not have the same behaviors in different applications [3,7,9,10,17].

There are different production methods for both HAp types: hydrothermal, mechano-chemistry, microwave irradiation, precipitation, sol–gel, hydrolysis, and micro-emulsion methods, among others, that have been used to obtain synthetic HAp [19]. In the natural HAp case, calcination, chemical, and thermal treatments have been used to remove the organic material in order to prevent infections, disease transfer, and immunological defensive reactions [3,8,18,20]. In most cases, bovine bone has been used as the HAp source for medical applications [10].

N.A.M. Barakat et al. [3] proposed three methodologies to clean bovine bone in order to establish a good process to eliminate the organic materials present in a sample. This study showed that by means of the thermal decomposition treatment produced carbonate-free HAp with better crystallinity than both the subcritical and alkaline treatments. On the other hand, D. Tadic and M. Epple [12] reported a complete study of different types of commercial calcium phosphates used in bone substitution from different sources (synthetic, animal and human), and the manufacturing processes. They reported that in some cases there are different HAp phases depending on the sample, e.g. tricalcium phosphate (TCP), octacalcium phosphate (OCP), calcium oxide (CaO), and in some cases, organic material like collagen and bioactive.

In this paper a comparison between the physicochemical properties of HAp obtained from bovine bone (bio-HAp) and commercial-HAp is reported. Three samples obtained from bovine bone by means of different treatments: *defat*, *alkaline*, and *calcined*, and five commercial samples obtained from companies and universities: *NIST*, *sigma*, *apafill G*, *coralina*, and *biograft*, were studied in order to establish the differences among the samples. By using TG analysis the mass loss as a function of the temperature was obtained in order to determine the presence of water and organic material in the samples. The structural characterization was performed by using XRD and FTIR techniques. The presence of HAp phase, the crystallite quality, as well as crystallinity percentage were determined by XRD. FTIR was used to identify the corresponding functional groups of HAp, and also to identify if carbonates and organic material are present. SEM analysis was performed in order to determine the morphology of the samples. Elemental analysis was carried out with ICP-OES in order to establish the mineral content in the samples.

2. Material and methods

8 different bio-HAp and commercial-HAp samples were studied. The bio-HAp group was comprised of 3 biological samples obtained from bovine bone using different treatments: 1) Treatment to remove fat: *defat*, 2) Alkali treatment: *alkaline*, and 3) Thermal treatment: *calcined*. All these samples were obtained from cortical bovine bones (2 years old) collected from the local slaughterhouse (folio number SDA-537295, 2011).

The commercial-HAp group comprised of 5 samples from different sources: 1) 1400 standard of bone ash certified by the National Institute of Standards & Technology: *NIST*, 2) Commercial-HAp from Sigma Aldrich (289396-synthetic): *sigma*, 3) Apafill G (Reg. No. 76LYC – synthetic, Centro de Biomateriales of La Habana University–Biomat): *apafill G*, 4) Coralina (HAP-200 – Reg. No. 47.174.92 – marine corals, Centro Nacional de Investigaciones Científicas – La Habana, Cuba): *coralina*, and 5) Biograft (Ref. 16140301, SN. 806330, LOT. DR-0005-08, human bone powder 1 cc): *biograft*, were analyzed.

2.1. Bone cleaning process

One of the most important procedures to obtain pure HAp from biological sources is the bone cleaning process; it aims to remove organic compounds such as fat and protein. In order to prepare bio-samples (bio-HAp), the first step in all cases was to cut the bone into smaller pieces and manually remove adhering soft tissue. Thereafter, the fluids in bone, marrow, and any remaining soft tissue were eliminated by boiling these small pieces of bone in deionized water during 30 min. The bone was then subjected to vacuum drying and a milling process using a stainless steel mill (Oster-USA) until powder was fine enough to pass through a mesh 100 (149 μm) sieve. After that, the three different processes mentioned above: *defat*, *alkaline*, and *calcined* were carried out respectively.

Process 1 – Defat: this consists in the removal of fat from the bone with solvents; firstly, the bone powder was treated with petroleum ether with constant agitation at 30 °C and then it was air-dried. After this step, the dried bone powder was immersed in acetone under ultrasound for 2 h, and after that, the powder was dried in a vacuum oven at 1.33 Pa and 70 °C for 5 h.

Process 2 – Alkaline: the bone powder was treated with sodium hydroxide solution at 8% p/v changing pH and temperature in order to eliminate proteins present in the bone. The powder was dried in a vacuum oven at 1.33 Pa and 70 °C for 5 h.

Process 3 – Calcined: the bone powder sample was heated from room temperature to 400 °C using a heating rate of 0.4 °C/min, and then from 400 to 900 °C using a heating rate of 1.4 °C/min. It was kept at this temperature for 3 h. The first ramp was to eliminate the organic materials without promoting the generation of carbonate phases; the second part of the ramp was to obtain the desirable HAp quality [8]. These temperatures ensure both the presence of the HAp phase, and that there will not be any organic material remaining [8].

All bio-samples were obtained after basic cleaning process. After the cleaning, samples were subject to different processes as follow: *defat* sample consist of bone with process 1, *alkaline* sample obtained after apply process 1 and process 2, and *calcined* sample obtained after apply process 1 and process 3.

2.2. Commercial sample preparation

The particle size of commercial samples was reduced until they passed through a mesh 100 (149 μm) sieve. In all cases, the samples were milled in an Agatha mortar.

2.3. Thermal behavior: TG analysis

The thermogravimetric curves and their derivative in relation to temperature were obtained by using TG Q500 equipment (TA Instruments). The sample mass was 12.0 ± 1.0 mg of each sample and these were placed in the platinum crucible of thermobalance (TA

Instruments, USA). The samples were heated from room temperature to 800 °C, at a heating rate of 10 °C/min; the measures were carried out in a constant N_2 flow. The TG data was processed using the Universal Analysis 2000 TA software.

2.4. Phase composition: XRD

X-ray diffraction was used to determine the presence of crystalline phases in the bio and commercial dry samples. Powder samples (mesh 100) were densely packed in an Al holder. X-ray diffraction patterns of the samples were carried out on a Rigaku Miniflex diffraction instrument operating at 35 kV, 15 mA with Cu K_α radiation wavelength of $\lambda = 1.5406$ Å. Diffractograms were obtained from 10 to 70° on a 2θ scale with a step size of 0.02°. The software used to analyze the spectrum was MDI Jade 5.0 (free version).

2.5. Functional groups: FTIR analysis

In order to obtain the functional groups present in the bio- and commercial-HAp samples FTIR Spectrum GX (Perkin Elmer) apparatus was used. Two milligrams (2 mg) of each sample was mixed with 98 mg of KBr (Potassium Bromide) powder. The Infrared spectra were measured in Medium Infrared (MIR) between 400 and 4000 cm^{-1} with a resolution of 4 cm^{-1}.

2.6. Surface microstructure: SEM

Morphologic analysis of all samples was carried out in a Jeol JSM 6060LV Scanning Electron Microscope. The analysis was performed using 20 kV electron acceleration voltages. Prior to the analysis, the samples were fixed on a copper specimen holder with carbon tape and covered with gold thin film in order to make them conductive before testing.

2.7. Elemental composition: ICP-OES

This technique was used to analyze the elemental composition in both the commercial and bio samples. Thermo iCAP 6500 Duo View equipment was used. 0.1 g of each sample was digested in nitric acid (Baker 69–70%) and it was made by triplicate. Upon return to the ground state, the elements excited by the argon plasma were then identified by their characteristic emission spectra. Emission intensity was then converted to elemental concentration by comparing to a standard curve.

3. Results and discussion

3.1. Thermal degradation analysis

TG is an excellent tool to determine the different thermal changes that take place in samples associated with the degradation of different phases (organic and inorganic). Fig. 1a, b show the mass loss as a function of the temperature in both the bio- and commercial-HAp samples respectively, and Fig. 1c shows the weight loss and its derivative behavior in the *defat*, *alkaline*, and *biograft* samples. As it is well known, one of the most important points in the case of HAp used in medical or dental applications is its degree of safety that is directly related to the absence or harmlessness of organic materials. Fig. 1a shows the bio samples:

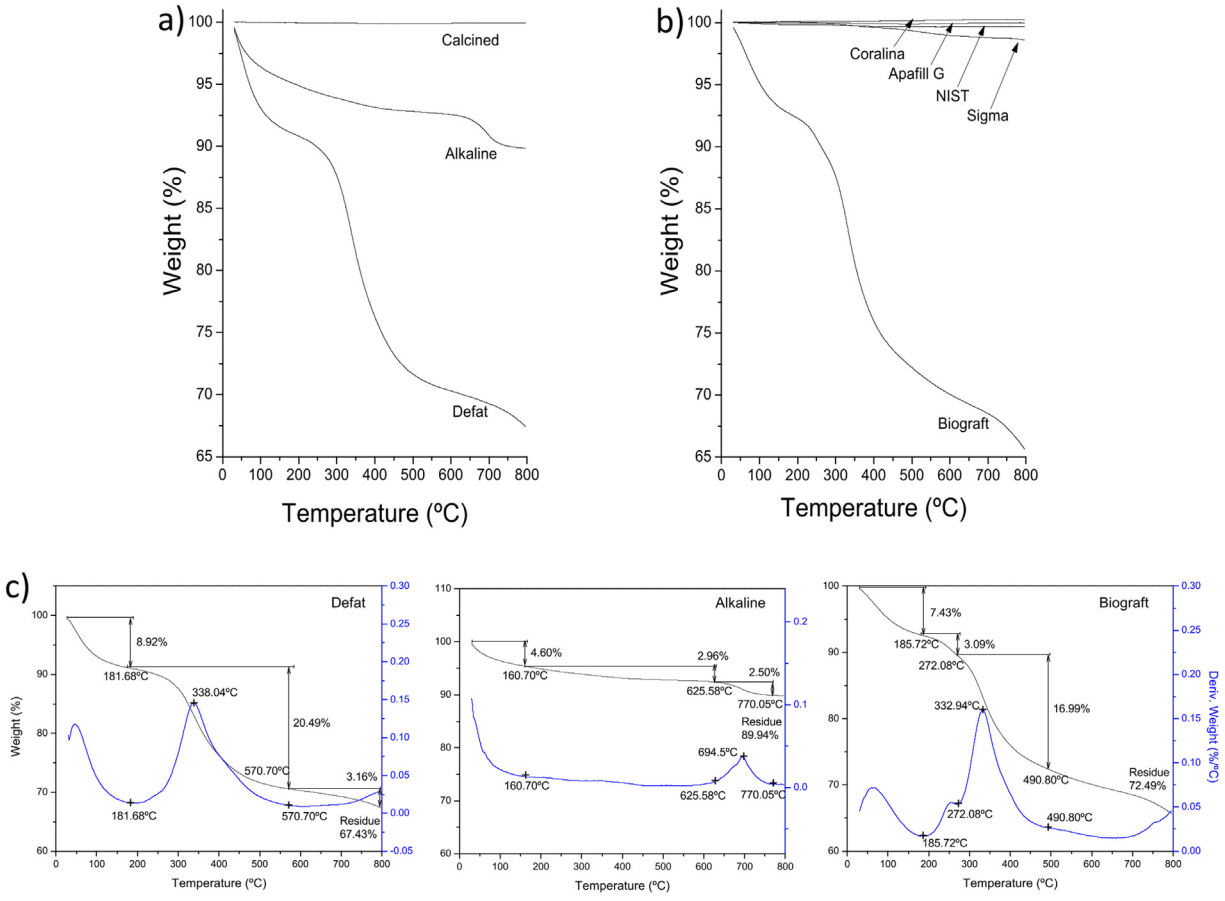

Fig. 1. Thermogravimetric curves of a) bio-HAp, b) commercial-HAp, and c) weigh loss and its derivate of *defat*, *alkaline* and *biograft* sample.

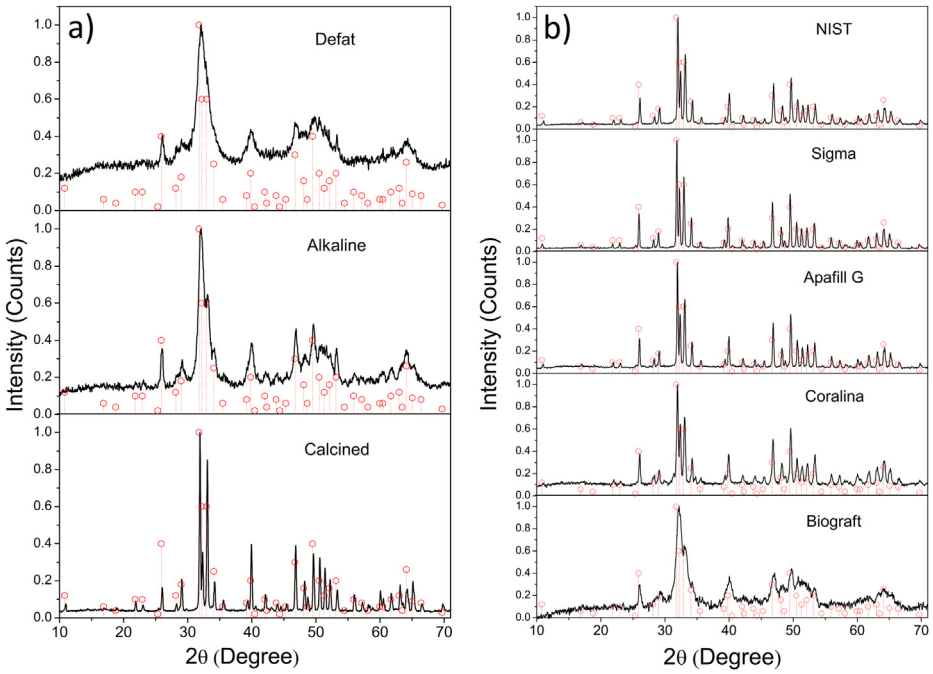

Fig. 2. X-ray diffraction patterns for a) bio-HAp and b) commercial-HAp.

Table 1
FWHM values from bio- and commercial-HAp samples for the main planes.

	Sample	(002)	(211)	(112)	(300)	(310)
Bio-HAp	*Defat*	0.50106	0.68826	0.66585	0.9793	0.82818
	Alkaline	0.38338	0.19616	0.72203	0.56995	0.739
	Calcined	0.22018	0.21457	0.18268	0.21872	0.22318
Commercial-HAp	*NIST*	0.18732	0.19772	0.18241	0.20933	0.24003
	Sigma	0.19475	0.19719	0.18782	0.20712	0.22452
	Apafill G	0.19511	0.19288	0.1873	0.19788	0.19492
	Coralina	0.22652	0.23746	0.1772	0.22182	0.21774
	Biograft	0.333	0.67429	0.27997	0.6047	1.00178

the *calcined* sample exhibited only around 1% of matter loss that is directly related to the moisture content, while the *alkaline* sample showed a loss of mass of 10.06% (4.60% moisture, and 5.46% corresponded with some fractions of fat and protein). A loss of 32.57% (moisture, fat, and protein) was found in the *defat* sample. On the other hand, Fig. 1b shows that the commercial samples did not exhibit a significant mass loss (around 1–3%): the same result as was found in the *calcined* sample (Fig. 1a), this is related with moisture content. However, in the *biograft* case, there was a loss of mass of 27.51% mass loss (moisture, fat, and protein). According to this TG analysis, it is clear that this commercial sample still has an important amount of organic compounds. Fig. 1c shows the changes in weight as a function of the temperature as well as its first derivative for *defat*, *alkaline*, and *biograft* samples. The *defat* and *biograft* samples exhibited the most significant changes above 200 °C; this may be due to the degradation of organic material [21].

According to L.F. Lozano et al. [21], the changes in the loss of mass located between 220 and 570 °C correspond with the degradation and combustion processes of collagen. In the case of the *defat* sample these processes occurred between 180 and 570 °C. Meanwhile, the *biograft* sample showed this phenomena but presented two peaks within this range of temperature: one located at 272 °C, which is related to the collagen degradation and the second located at 333 °C which corresponds with protein denaturalization or de-branched. Finally, the *alkaline* sample did not show this behavior, but it presented a peak around 695 °C that corresponds to the dissociation of carbonated apatite in the calcium carbonated form ($CaCO_3$) [11,12]. This result is indicative that the alkaline process removed a part of the organic matrix.

3.2. Structural characterization

3.2.1. Crystalline phases presence

XRD is an excellent technique to determine the crystalline phases present in any sample, and it is indicative of the chemical structure. Fig. 2a and b show the XRD patterns of the bio and commercial samples, respectively. In these figures, the vertical dash lines are included that correspond to the comparison with JCPD file No. 09-432 of pure HAp. All samples in Fig. 2 consist of a pure HAp phase. The XRD patterns in Fig. 2 show the most intense peaks corresponding to (002), (211), (112), (300), and (310) planes. The crystallinity was established using the full width at half maximum (FWHM) value of the main XRD peaks as (002), (211), (112), (300), and (310) (Table 1). This parameter is inversely proportional to the average crystalline size according to the Scherrer equation [12,22,23]; indicating that for FWHM small values, the crystallite size increases as well as the crystallinity. From XRD patterns the crystallinity percent was determine and it is shown in Table 2. This parameter defines minimal medical requirements for coatings according to the ASTM and ISO norms [24].

Table 2
Crystallinity percent of bio- and commercial-HAp.

Sample	*Defat*	*Alkaline*	*Calcined*	*NIST*	*Sigma*	*Apafill G*	*Coralina*	*Biograft*
Crystallinity (%)	66.81	80.21	88.35	83.72	91.76	73.98	84.07	61.64

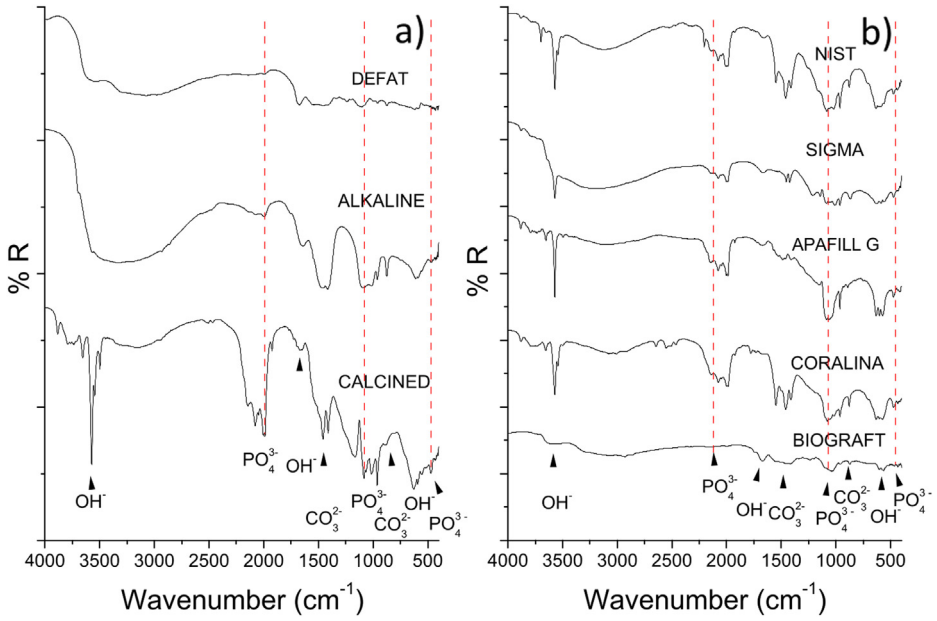

Fig. 3. Infrared spectra of a) bio-HAp and b) commercial-HAp.

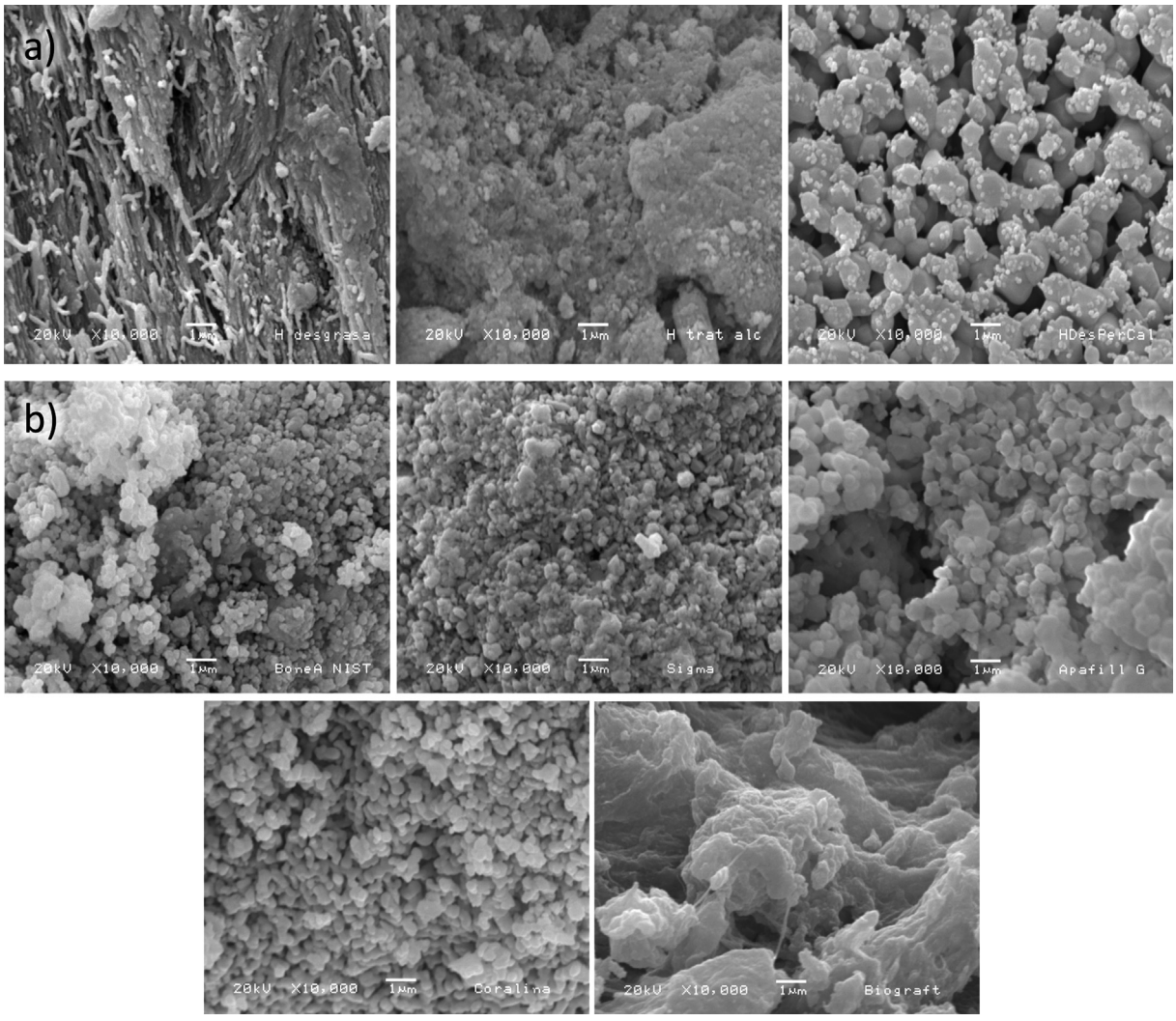

Fig. 4. SEM micrographs of a) bio-HAp (*defat – alkaline – calcined*) and b) commercial-HAp (*NIST – sigma – apafill G – coralina – biograft*), respectively.

In the commercial-HAp samples, all of them have similar high crystallinity quality, except for the *biograft* sample. The *biograft* had similar crystallinity quality to the *defat* and *alkaline* samples whose behavior resembled that found in the TG analysis.

In Fig. 2a *calcined* sample exhibited the most defined peaks in comparison with the *defat* and *alkaline* samples. According to FWHM values obtained for these samples, shown in Table 1, the *calcined* sample presents the best crystallinity quality followed by the *alkaline* and *defat* samples. Moreover, the commercial-HAp samples, except *biograft*, have a high crystallinity and presented well-defined peaks as in the *calcined* sample (bio-HAp) as it is shown in Fig. 2b. The behavior of the *defat*, *alkaline*, and *biograft* samples could be associated with the organic material present in the samples. The *calcined*, *NIST*, *sigma*, *apafill G*, and *coralina* samples had similar FWHM values in each analyzed plane, while the values of the *defat*, *alkaline*, and *biograft* samples had differences among the studied planes.

3.2.2. Functional groups

In order to obtain more information about the components and the functional groups present in the samples, FTIR spectroscopy was used as a complementary technique to XRD. The IR spectra of all the samples are shown in Fig. 3. The IR spectrum of each sample shows the characteristic bands of the HAp structure. The absorption peaks located at 3571 cm^{-1} (ν_3), and 632 cm^{-1} (ν_L) were attributed to the structural hydroxyl groups (OH^-) and the peaks located at 1103 and 1040 cm^{-1} (ν_3), 960 cm^{-1} (ν_1), 602 and 564 cm^{-1} (ν_4), and 474 cm^{-1} (ν_2) correspond with the phosphate group (PO_4^{3-}) [25]. These characteristic bands are typical of hydroxyapatite and these were present in the IR spectrum of the samples with different intensities and broad of peaks. In some samples a trace of water molecule incorporated into the structure appears with a broad band and a variable intensity between the 3200–3600 cm^{-1} (stretching mode) and 1600–1700 cm^{-1} (bending mode) ranges [11].

Fig. 3a shows that in the *calcined* case, the absorption bands are more defined in comparison with the other bio-HAp samples, indicating that the *calcined* sample had a high degree of crystallinity as was shown using XRD in Fig. 2a; also it confirms the removal of the organic matrix [6]. In Fig. 3b, commercial-HAp samples show the typical HAp spectrum well defined as in the *calcined* sample, except in the *biograft* case. The *biograft* sample presented non-well defined peaks that correlate with its low degree of crystallinity. The same result was found for the *defat* sample.

On the other hand, the IR spectra presented a carbonate contribution (CO_3^{2-}) at 1470 cm^{-1} (ν_3), and 860 cm^{-1} (ν_2) in all cases [24]. The *defat* and *biograft* samples presented absorption bands at 1549 cm^{-1} that correspond to the amide II (60% N–H bending mode, and 40% C–N stretching mode), and 1240 cm^{-1} that correspond to the amide III (30% C–N stretching mode, 30% N–H bending mode, 10% C=O stretching mode, 10% O=C–N bending mode and 20% other) [6,26], corroborating the presence of organic material in these samples.

3.3. Morphological characterization

SEM analysis is an excellent tool to study the morphology of the samples at a microscopic level. Fig. 4 shows the SEM images of the studied samples. The morphology differences of the bio-HAp samples are shown in Fig. 4a; the *defat* sample presents a dense surface, which corresponds with the presence of organic material. In the *alkaline* sample the surface begins to show some pores but is still dense though less than the defatted sample. In the *calcined* case, the surface presents the characteristic morphology of HAp without organic material [8]. The *calcined* sample shows a surface with pores that corresponds to the elimination of collagen (organic material) with the heat treatment. According to C.Y. Ooi et al. [8], this behavior corresponds to an interconnecting porous network that is suitable for bone in-growth.

In the commercial-HAp cases the morphology of all samples are similar to the *calcined* sample. However, the commercial samples have a smaller pore size (the diameter of the pore measured in SEM images is based on the cross section), as seen in Fig. 4b, this

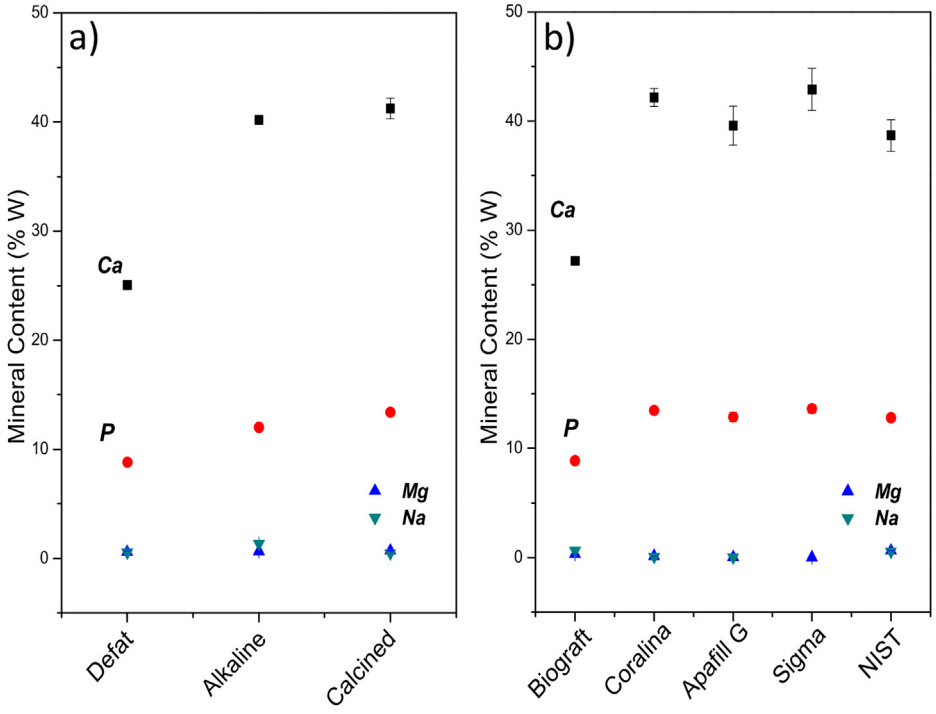

Fig. 5. Major elemental content in a) bio-HAp and b) commercial-HAp samples.

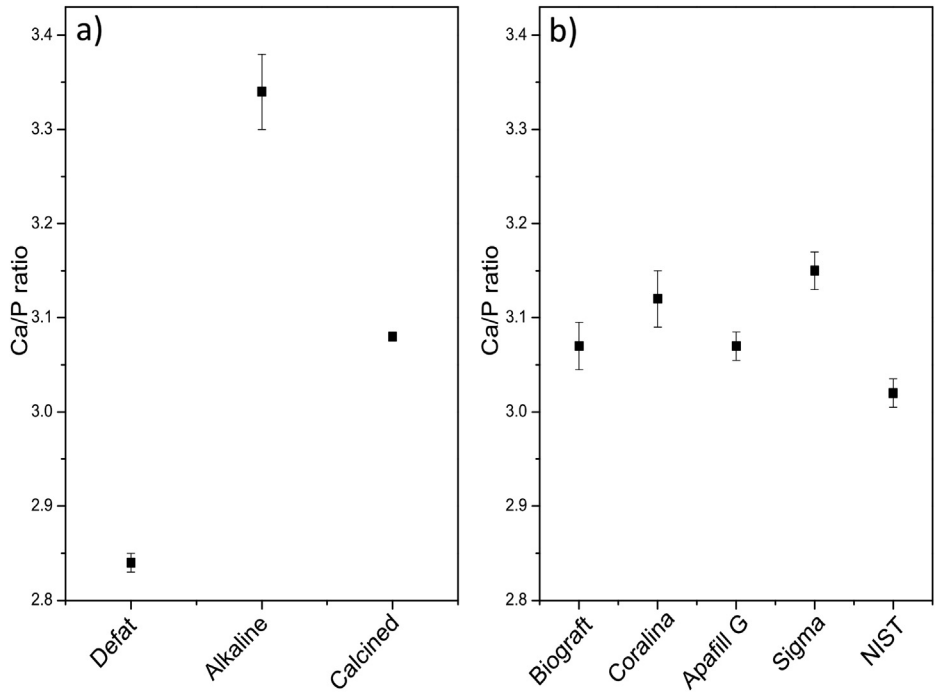

Fig. 6. Ca/P ratio of a) bio-HAp and b) commercial-HAp samples.

Table 3
Minor elemental content in bio- and commercial-HAp samples.

Sample		Al (mg/Kg)	Ba (mg/Kg)	Cu (mg/Kg)	Fe (mg/Kg)	K (mg/Kg)	Mn (mg/Kg)	Ni (mg/Kg)	Zn (mg/Kg)
bio-HAp	*Defat*	6.6 ± 0.21	294.08 ± 4.74	1.07 ± 0.76	31.36 ± 0.1	345.27 ± 5.06	–	–	79.46 ± 0.98
	Alkaline	6.66 ± 0.32	241.99 ± 1.56	5.22 ± 2.01	83.33 ± 14.5	–	–	–	135.81 ± 0.25
	Calcined	20.01 ± 1.27	265.58 ± 13.15	9.05 ± 0.22	42.71 ± 0.45	228.14 ± 6.84	1.25 ± 0.04		139.38 ± 6.05
Commercial-HAp	*NIST*	270.53 ± 4.45	240.76 ± 5.16	2.7 ± 0.01	645.45 ± 17.18	–	17.44 ± 0.11	5.8 ± 0.54	180.87 ± 3.38
	Sigma	5.72 ± 0.6	–	–	11.57 ± 1.45	–	–	–	3.66 ± 0.08
	Apafill G	103 ± 2.9	150.3 ± 5.02	15.33 ± 0.46	137.17 ± 4.86	–	59.73 ± 1.97	–	24.88 ± 1.16
	Coralina	14.29 ± 0.28	8.49 ± 0.11	3.98 ± 0.88	25.98 ± 0.33	–	–	–	6.94 ± 0.26
	Biograft	6.62 ± 0.92	1.62 ± 0.07	–	16.69 ± 1.42	–	–	–	119.05 ± 2.64

behavior is not present in the *biograft* sample. The morphology of the *biograft* presents a dense surface along with the *defat* (Fig. 4a) that confirms the presence of organic material.

3.4. Elemental composition

The elementary composition of the samples was investigated with ICP-OES. Results of minor and major elemental content are shown in Fig. 5 and listed in Table 2, respectively. The main components of the samples are calcium and phosphorus and their Ca/P ratio are shown in Fig. 6. As minor components of the major elemental content in the samples there are magnesium and sodium. The samples showed only slight variations in the minor components of the major elemental content in the results. Fig. 5a and b shows that calcium and phosphorous are the major elemental content present in the samples and their variations depend on the source [10]. Moreover, traces of aluminum, barium, copper, iron, potassium, manganese, nickel, and zinc were detected as indicated in Table 2.

It should be emphasized that the samples from a natural source exhibited the mineral traces own of bone, as it was expected; however, none of the following elements were found in the *sigma* sample: magnesium, barium, copper, potassium, manganese, and nickel. This indicates that this sample was obtained by a chemical process (Table 3).

The Ca/P ratios, in Fig. 6, do not show a tendency. In general, the Ca/P ratio values are above 3, except for the *defat* sample [8]. Fig. 6a shows Ca/P ratios between 2.8 and 3.4 and Fig. 6b presents Ca/P ratios between 3 and 3.2 that correspond with non-stoichiometric HAp's. This variation of the Ca/P ratio is correlated with the ionic interchange in the HAp structure and due to presence of the other minerals or the coexistence of other minor calcium phases. The most common calcium phases present in the HAp samples are the calcium oxide, hydroxide or carbonate [10].

4. Conclusions

The *calcined*, *NIST*, *sigma*, *apafill G*, and *coralina* did not show thermal changes related with the organic phases and calcium carbonate after TG analysis. Organic degradation in the *defat* and *biograft* samples was found. Three bovine bone samples under the *defat*, *alkaline*, and *calcined* processes were compared. After the calcination process the organic material was removed. It was found that this process is an appropriate manner to obtain crystalline HAp with the minor and major elements that appear in natural bone tissue. According to XRD analysis both the *defat* and *biograft* samples, in comparison with the other samples, have the lowest crystallinity quality and crystallinity percentage. The functional groups own of HAp in bio and commercial samples were found. The samples presented a carbonate contribution and it was not detected in XRD analysis. Absorption bands in 1549 and 1240 cm^{-1} corresponding to the amide II and amide III respectively, were present in the *defat* and *biograft* samples. A dense surface on both the *defat* and *biograft*

samples was found in SEM micrographs. In *calcined*, *NIST*, *sigma*, *apafill G*, and *coralina* the interconnecting porous networks are present. The surface of the *alkaline* sample showed a transition behavior between dense and porous morphology. According to ICP-OES analysis calcium and phosphorous are both present as a major elemental content while magnesium and sodium are present as minors of the major elemental content. Bio-HAp with similar physicochemical properties to commercial-HAp was obtained after applying the *alkaline* and *calcined* processes. The temperature during the calcined process is an important factor as a high temperature of calcination forms different HAp phases.

Acknowledgments

Astrid L. Giraldo wants to thank Consejo Nacional de Ciencia y Tecnología (CONACYT) for the financial support of her Ph. D. thesis. Authors acknowledge the help of Reina Araceli Mauricio Sánchez and Carolina Muñoz for FTIR and ICP measurements, respectively. Also we acknowledge to Charlotte Elizabeth Connabeer for her support in the English revision of this paper. Finally, E. M. Rivera-Muñoz and B. M. Millán Malo acknowledge the support of Project DGAPA-UNAM PAPIIT IN107311.

References

[1] M. Hernández-Urbiola, A.L. Giraldo-Betancur, D. Jimenez-Mendoza, E. Pérez-Torrero, I. Rojas–Molina, M.A. Aguilera-Barreiro, C. Muñoz-Torres, M.E. Rodríguez-Garcia, Mineral content and physicochemical properties in female rats bone during growing stage, in: M. Akhyar-Farrukh (Ed.), Atomic Absorption Spectroscopy, INTech, 2012, pp. 202–220.
[2] M.M. Stevens, Biomaterials for bone tissue engineering (Review), Mater. Today 11 (2008) 18–25.
[3] N.A.M. Barakat, K.A. Khalil, F.A. Sheikh, A.M. Omran, B. Gaihre, S.M. Khil, H.Y. Kim, Physicochemical characterizations of hydroxyapatite extracted from bovine bones by three different methods: extraction of biologically desirable HAp, Mater. Sci. Eng. C 28 (2008) 1381–1387.
[4] E.M. Rivera-Muñoz, Hydroxyapatite-based materials: synthesis and characterization, in: R. Fazel-Rezai (Ed.), Biomedical Engineering: Frontiers and Challenges, INTech, 2011, pp. 75–98.
[5] C.P. Yoganand, V. Selvarajan, O.M. Goudouri, K.M. Paraskevopoulos, Junshu Wu, Dongfeng Xue, Preparation of bovine hydroxyapatite by transferred arc plasma, Curr. Appl. Phys. 11 (2011) 702–709.
[6] M. Younesi, S. Javadpour, M.E. Bahrololoom, Effect of heat treatment temperature on chemical compositions of extracted hydroxyapatite from bovine bone ash, J. Mater. Eng. Perform. 20 (8) (2011) 1484–1490.
[7] D.S.R. Krishna, C.K. Chaitanya, S.K. Seshadri, T.S.S. Kumar, Fluorinated hydroxyapatite by hydrolysis under microwave irradiation, Trends Biomater. Artif. Organs 16 (2002) 15–17.
[8] C.Y. Ooi, M. Hamdi, S. Ramesh, Properties of hydroxyapatite produced by annealing of bovine bone, Ceram. Int. 33 (2007) 1171–1177.
[9] G. Goller, F.N. Oktar, S. Agathopooulos, D.U. Tulyaganov, J.M.F. Ferreira, E.S. Kayali, I. Peker, Effect of sintering temperature on mechanical and microstructural properties of bovine hydroxyapatite (BHA), J. Sol Gel Sci. Technol. 37 (2006) 111–115.
[10] S. Joschek, B. Nies, R. Krotz, A. Göpferich, Chemical and physicochemical characterization of porous hydroxyapatite ceramics made of natural bone, Biomaterials 21 (2000) 1645–1658.
[11] E. Kusrini, M. Sontag, Characterization of X-ray diffraction and electron spin resonance: effects of sintering time and temperature of bovine hydroxyapatite, Radiat. Phys. Chem. 81 (2012) 118–125.
[12] D. Tadic, M. Epple, A thorough physicochemical characterization of 14 calcium phosphate-based bone substitution materials in comparison to natural bone, Biomaterials 25 (2004) 987–994.
[13] P. Ducheyne, S. Radin, L. King, The effect of calcium phosphate ceramic composition and structure on *in vitro* behavior. I. Dissolution, J. Biomed. Mater. Res. 27 (1993) 25–34.
[14] D. Belluci, A. Sola, M. Gazzarri, F. Chiellini, V. Cannillo, A new hydroxyapatite-based biocomposite for bone replacement, Mater. Sci. Eng. C 33 (2013) 1091–1101.
[15] S.V. Dorozhkin, Bioceramics of calcium orthophosphates (Review), Biomaterials 31 (2010) 1465–1485.
[16] E. Schepers, M. de Clercq, P. Ducheyne, R. Kempeneers, Bioactive glass particulate material as a filler for bone lesions, J. Oral Rehabil. 18 (1991) 439–452.
[17] C.P. Yoganand, V. Selvarajan, J. Wu, D. Xue, Processing of bovine hydroxyapatite powders and synthesis of calcium phosphate silicate glass ceramics using DC thermal plasma torch, Vacuum 83 (2009) 319–325.
[18] W.J. Lo, D.M. Grant, M.D. Ball, B.S. Welsh, S.M. Howdale, E.N. Antonov, V.N. Bagratashvili, V.K. Popov, Physical, chemical and biological characterization of pulsed laser deposited and plasma sputtered hydroxyapatite thin films on titanium alloy, J. Biomed. Mater. Res. 50 (2000) 536–545.
[19] E.M. Rivera-Muñoz, R. Velázquez, J.L. Cabrera-Torres, Morphological analysis of hydroxyapatite particles obtained by different methods, Mater. Sci. Forum 638–642 (2010) 681–686.
[20] F.H. Lin, C.J. Liao, K.S. Chen, J.S. Sun, Preparation of a biphasic porous bioceramic by heating bovine cancellous bone with $Na_4P_2O_7 \cdot 10H_2O$ addition, Biomaterials 20 (1999) 475–484.
[21] L.F. Lozano, M.A. Peña-Rico, A. Heredia, J. Ocotlán-Flores, A. Gómez-Cortés, R. Velázquez, I.A. Belío, L. Bucio, Thermal analysis study of human bone, J. Mater. Sci. 38 (2003) 4777–4782.
[22] R. Velazquez-Hernandez, I. Rojas-Rodriguez, J. Carmona-Rodríguez, S. Jiménez-Sandoval, M.E. Rodriguez-Garcia, Structural and photocarrier radiometric characterization of $Cu_x(CdTe)_yO_z$ thin films, Thin Solid Films 519 (2011) 2135–2140.
[23] A. Ruksudjarit, K. Pengpat, G. Rujijanagul, T. Tunkasiri, Synthesis and characterization of nanocrystalline hydroxyapatite from natural bovine bone, Curr. Appl. Phys. 8 (2008) 270–272.
[24] Y. Yang, K.H. Kim, J.L. Ong, A review on calcium phosphate coatings produced using a sputtering process–an alternative to plasma spraying, Biomaterials 26 (2005) 327–337.
[25] A. Costescu, I. Pasuk, F. Ungureanu, A. Dinischiotu, M. Costache, F. Huneau, S. Galaup, P. Le Coustumer, D. Predoi, Physico-chemical properties of nanosized hexagonal hydroxyapatite powder synthesized by sol–gel, Dig. J. Nanomater. Bios. 5 (2010) 989–1000.
[26] B. Stuart, Infrared Spectroscopy: Fundamentals and Applications, John Wiley & Sons, Ltd, 2004.